# Accidental predissociation phenomena in the $E\ ^1\Pi$, $v=0$ and $v=1$ states of $^{12}C^{16}O$ and $^{13}C^{16}O$

Patrice Cacciani,[a] Wim Hogervorst, and Wim Ubachs
*Laser Centre Vrije Universiteit, De Boelelaan 1081, 1081 HV Amsterdam, the Netherlands*

(Received 12 December 1994; accepted 23 February 1995)

We have studied $v=0$ and $v=1$ levels of the $E\ ^1\Pi$ state of CO in excitation from the ground state by one- and two-photon transitions, thus probing $e$ and $f$ $\Lambda$-doublet components. New accidental predissociations were found in the $E\ ^1\Pi$, $v=0$ state for high $J$ values ($J_e=41$, 44 for $^{12}C^{16}O$ and $J_e=41$, 50 for $^{13}C^{16}O$). The predissociation phenomenon in the $E\ ^1\Pi$, $v=1$ state at $J=7$ was reinvestigated and for both $e$ and $f$ components also $J=9$, 10, and 12 were found to be perturbed. Perturbations by all three spin components of a $k\ ^3\Pi$, $v=5$ state were deduced. Furthermore the accidental predissociation in $E\ ^1\Pi$, $v=0$ $J_e=31$ was reinvestigated. Measurements of spectral line shifts were modeled assuming a spin-orbit coupling between $E\ ^1\Pi$ and the $^3\Pi_1$ component of the $k\ ^3\Pi$ state. Relative predissociation lifetimes of $k\ ^3\Pi$, $v=3$ and 5 with respect to $E\ ^1\Pi$, $v=0$ and $v=1$ are deduced from an analysis of observed intensity effects. For the $E\ ^1\Pi$, $v=1$ state rotational state dependent lifetimes were determined at low-$J$ values. Line positions of CO lines were calibrated on an absolute frequency scale within 0.05 $cm^{-1}$ against the tellurium and iodine standard in the visible. Accurate molecular constants for the $E\ ^1\Pi$, $v=0$ and $v=1$ states are determined for both $^{12}C^{16}O$ and $^{13}C^{16}O$. The $E\ ^1\Pi$, $v=1$ state of $^{12}C^{17}O$ is observed for the first time. © *1995 American Institute of Physics.*

## I. INTRODUCTION

The photodissociation of carbon monoxide in the vacuum ultraviolet (vuv) wavelength range 90–115 nm is a key parameter governing the chemical dynamics of the interstellar medium.[1,2] The limits of the relevant wavelength range correspond to the ionization potential of atomic hydrogen and the first dissociation limit of CO (89 460 $cm^{-1}$). Letzelter *et al.*[3] established that the photodissociation mechanism does not involve direct excitation to a repulsive state, but rather occurs via absorption in rotationally resolved discrete bands which exhibit predissociation. In view of its astrophysical importance a number of detailed spectroscopic investigations on CO in the vuv range have been performed in recent years, by making use of classical spectrographs,[4,5] synchrotron sources[6–8] and laser sources.[9–11] The $E\ ^1\Pi$ and $C\ ^1\Sigma^+$ states, correlating with $3p\pi$ and $3p\sigma$ electronic orbitals have the largest integrated absorption cross sections among the predissociated states and therefore are crucial for the understanding of the photochemistry of CO in the interstellar medium.

The $E\ ^1\Pi - X\ ^1\Sigma^+$ transition of CO was first observed by Hopfield and Birge[12] and later analyzed in higher resolution by Tilford *et al.*[13] An accidental predissociation of the $E\ ^1\Pi$, $v=0$, $J=31$, $e$-parity level attracted interest throughout the years. After a photographic study of Simmons and Tilford,[14] Klopotek and Vidal[15] employed a double resonance laser technique, while Amiot *et al.*[16] recorded near infrared Fourier-transform spectra of $E\ ^1\Pi - C\ ^1\Sigma^+$ and $E\ ^1\Pi - B\ ^1\Sigma^+$ transitions to investigate this phenomenon. No evidence for predissociation of the $J=31$, $f$-parity level was found and from these studies no identification of the perturber state could be deduced. A similar accidental predissociation was observed in both a spectrograph study[4] and a synchrotron study[7] for the $E\ ^1\Pi$, $v=1$, $J=7$ level, for both $e$ and $f$ parity levels and both $^{12}C^{16}O$ and $^{13}C^{16}O$ isotopes.

In two recent publications by Baker *et al.*[11,17] the issue of the accidental predissociations in the $E\ ^1\Pi$ state was addressed. First, two-photon laser excitation revealed the predissociation behavior of both $e$ and $f$ levels for $E\ ^1\Pi$, $v=1$ in several isotopes including $^{12}C^{18}O$, $^{13}C^{16}O$, and $^{13}C^{18}O$.[11] Second, in a vuv spectrographical study a vibrational progression $k\ ^3\Pi$, $v=2$, 3 and 5 was observed in excitation from the ground state.[17] This allowed reassignment of the vibrational progression observed by Wan and Langhoff[18] in CO excited by electron bombardment. Vibrational levels $v=1$ and 2 of $k\ ^3\Pi$ were observed in double-resonance excitation by Mellinger and Vidal,[19] who also deduced limiting values for their lifetimes. The location of the $k\ ^3\Pi$ levels provides an identification of the perturber state causing the above-mentioned accidental predissociations in the $E\ ^1\Pi$ state. The $E\ ^1\Pi$, $v=0$, $J_e=31$ is found to nearly coincide with the $k\ ^3\Pi_2$ $v=3$, $J=31$ level, while the $E\ ^1\Pi$, $v=1$, $J=7$ level nearly coincides with the $k\ ^3\Pi_0$ $v=5$, $J=7$ level. Also the $e-f$ parity dependences of the predissociation mechanism could be explained. Recently also an interaction between $B\ ^1\Sigma^+$, $v=2$ and $k\ ^3\Pi$, $v=0$ states was reported by Baker.[20]

In the present paper we present results of two different laser-based investigations of the $E\ ^1\Pi$, $v=0$ and $v=1$ states. First a $2+1$ resonantly enhanced multiphoton ionization (REMPI) technique was applied, similar to previous work by Hines *et al.*[21] and Baker *et al.*[11] Because we observed signals from samples of $^{12}C^{16}O$ and $^{13}C^{16}O$ heated to 1000 K new information on high-lying rotational states up to $J\approx 50$ was obtained. For $^{12}C^{16}O$ new accidental predissocia-

[a]Permanent address: Laboratoire Aimé Cotton, Bat 505 Campus d'Orsay, 91405 Orsay cedex, France.

 0021-9606/95/102(21)/8308/13/$6.00 

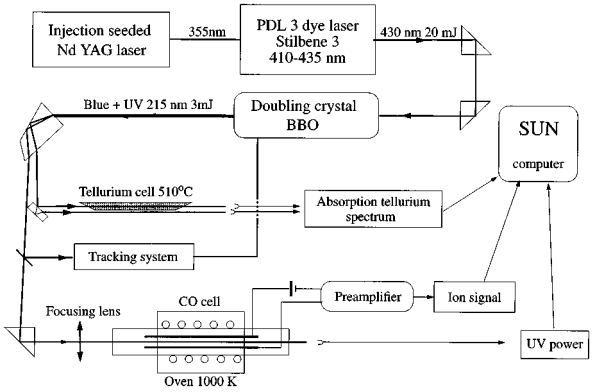


FIG. 1. Schematic drawing of the experimental setup used for the 2+1 REMPI measurements. Ultraviolet in the range 210–216 nm, obtained from a blue dye laser after frequency doubling in a BBO crystal, is focused into a sample of natural CO or $^{13}$C enriched CO at high temperatures and pressures of ≈3 Torr.

tions were observed at $J_e=41$ and 44 and similarly for $^{13}C^{16}O$ at $J_e=41$ and 50. These perturbations are attributed to $v=4$ and $v=5$ levels of the $k\ ^3\Pi$ state. In a second experiment coherent vuv radiation in the range 105–107 nm, produced by frequency tripling a frequency doubled dye laser, was used in combination with a molecular beam setup for Doppler-free measurements. As the relative intensities in 1 vuv+1 uv photoionization detection are very sensitive to predissociation effects,[10] new details on the predissociation of the $E\ ^1\Pi$, $v=1$, $J=7$ state could be revealed. Further proof of the triplet character of the perturber state is established as all three spin components of the $k\ ^3\Pi$ state are found to affect the rotational manifold of the $E\ ^1\Pi$, $v=1$ state. From a detailed analysis of linewidths, line shifts, and relative line intensities, lifetimes as a function of the rotational quantum state $J$ were determined for the $E\ ^1\Pi$, $v=1$ state. In both experiments the frequency is on-line calibrated against the tellurium or iodine reference spectrum and an accurate spectroscopic analysis could be performed for the $E\ ^1\Pi$ $v=0$ and $v=1$ states, resulting in high precision molecular constants.

## II. EXPERIMENTAL SETUP

The first experimental configuration, used for the 2+1 REMPI study of CO, is drawn in Fig. 1. The uv radiation (355 nm) of an injected-seeded NdYAG laser pumps a Stilbene 3 dye laser (PDL3) in the 420–432 nm range. This radiation is frequency doubled in a BBO crystal to obtain tunable uv radiation in the wavelength range of 210–216 nm with pulse energies of up to 3 mJ. The uv radiation is focused by a 25 cm lens in the center of a cell filled with 3 Torr of CO. The remaining blue radiation is used to register the absorption spectrum of tellurium from a separate cell heated at 510 °C for on-line frequency calibration.[22] Ultraviolet as well as blue laser energy are monitored on photodiodes for normalisation procedures averaging out shot-to-shot fluctuations in the REMPI signals and $Te_2$-reference spectrum.

The cell used for the REMPI study can be heated up to 1000 K. The elevated temperature allows observation of rotational values up to $J\approx 50$. The temperature is limited because of the occurrence of a discharge for $T>1000$ K. The ions are collected between two plates, where a 9 V bias voltage is applied, then the current is amplified and registered. Because of a continuous thermoelectronic current the pulsed REMPI signal is capacitively decoupled before amplification and recording.

The 2+1 REMPI method applied to static samples of CO is neither isotope selective nor Doppler free. Therefore, two different samples were studied: natural CO and a sample enriched in $^{13}$C. Although the isotopic purity of the two samples was specified better than 98.5% $^{12}C^{16}O$, respectively, $^{13}C^{16}O$ the spectral content was contaminated. Because of the wall-sticking effect of carbon monoxide on non-heated parts, the cell could not be efficiently evacuated. The effective isotopic purity obtained in the spectra is 90% for the $^{13}$C enriched sample and 95% for $^{12}C^{16}O$.

For absolute calibration purposes the tellurium absorption lines were fitted to Gaussian profiles and the well-resolved lines were assigned according to the $Te_2$ atlas.[22] The frequency scale was linearized to correct for small nonlinearities in the scan of the dye laser. After normalization for uv fluctuations the CO lines were also fitted to Gaussians. Typical linewidths in the 2+1 REMPI spectra are 1 $cm^{-1}$. The error in the determination of line positions can vary from 0.02 to 0.3 $cm^{-1}$ depending on the signal-to-noise ratio which decreases for the highest $J$ values. The intrinsic accuracy of the tellurium-frequency scale has been estimated to be better than 0.06 $cm^{-1}$ (after multiplication by four). The line positions obtained from computerized interpolation and their uncertainties were used in a least-squares fitting procedure to derive molecular constants.

A second experimental configuration involves a vacuum ultraviolet laser source, which was described in previous publications on the spectroscopy of CO in the range 90–100 nm.[9,10] Narrowband tunable vuv radiation is produced by generation of the third harmonic of a frequency-doubled dye laser near 630 nm in a pulsed gas jet. Efficiencies of various tripling gases were monitored and it was found that near 107 nm acetylene ($C_2H_2$) yielded the highest conversion efficiency, while near 105 nm CO was most efficient. In both cases it was verified that the vuv yield smoothly varied over the wavelength range required to cover the $E\ ^1\Pi - X\ ^1\Sigma^+(1,0)$ and (0,0) band spectra. Consequently, the intensity variations in the spectra cannot be attributed to wavelength dependent fluctuations in the vuv yield.

The vuv and uv beams perpendicularly cross a pulsed CO beam. Ions, produced by 1 vuv+1 uv photoionization, are mass selected by means of a time-of-flight zone and detected on an electron multiplier. By making use of multiple boxcar integrators spectra of different isotopic species could be recorded selectively and simultaneously. The high sensitivity of this setup allows to record spectra of $^{12}C^{16}O$, $^{13}C^{16}O$, $^{12}C^{18}O$, and even $^{12}C^{17}O$ from a natural sample of CO. The $^{13}$C enriched sample of CO, that was used for the 2+1 REMPI experiments and available only in limited quantities, was not sufficient to sustain a molecular beam expansion for the vuv experiment. Simultaneously with the vuv excitation spectra of CO the $I_2$-absorption spectrum was recorded in the visible wavelength range 630–635 nm at the

fundamental of the dye laser. Accurate frequency positions were determined from a computerized linearization and interpolation procedure and comparison with the $I_2$ standard.[23,24] Because the observed lineshapes in vuv excitation are symmetric and narrower (observed linewidth 0.4 $cm^{-1}$) the accuracy in the line positions (0.04 $cm^{-1}$) is better than in the 2+1 REMPI experiment.

## III. PREDISSOCIATION EFFECTS DERIVED FROM INTENSITY MEASUREMENTS

When a bound quantum state of a molecule couples to a continuum state, there is a certain probability that the molecule will dissociate upon excitation to this state. This phenomenon is called predissociation.[25] It reduces the lifetime of the state and may be observed as line broadening in any spectroscopic study, independent of the specific detection technique. The absorption cross section, however, when integrated over the line profile does not change, and therefore predissociation is not easily observed in absorption. Because of the competition between radiative and dissociative decay the fluorescence yield from predissociative states diminishes and consequently the effects of predissociation are more easily observed in emission studies.

Electronic predissociation may be caused by a coupling to a repulsive state, or to an intermediate state which itself is predissociative. In the first case there is a overall effect: all $J$ states of a rotational manifold are affected. In case of a coupling through an intermediate state, predissociation will become manifest for those $J$ states that nearly coincide with a perturbing level. This resonance feature is called accidental predissociation. It is important to note that the $E\ ^1\Pi$, $v=0$ and $v=1$ states are believed to undergo both overall and accidental predissociation effects.

In multiphoton ionization studies predissociation effects can be derived from line broadening effects. Isotope, rotational-state and parity-dependent predissociation rates of high lying states of CO were, e.g., determined in 1 xuv+1 uv photoionization studies.[9,10] In the case of $E\ ^1\Pi$, $v=0$ and $v=1$ states the decay rates, including radiative and predissociative channels, are estimated to be $10^9$ and $10^{10}$ $s^{-1}$, respectively.[4] The natural linewidth $\Gamma$ (in $cm^{-1}$) is related to the total decay rate $k$ and the excited state lifetime $\tau$ by

$$\Gamma = \frac{k}{2\pi c} = \frac{1}{2\pi c \tau}. \tag{1}$$

These rates would correspond to linewidth contributions of 0.005 and 0.05 $cm^{-1}$, respectively. The excited state lifetime $\tau$ can be determined from the observed linewidth. It requires deconvolution of the instrumental linewidth $\delta\nu_{\rm instr}$ from the observed width $\delta\nu_{\rm obs}$[10,26]

$$\Gamma = \delta\nu_{\rm obs} - \frac{(\delta\nu_{\rm instr})^2}{\delta\nu_{\rm obs}} \tag{2}$$

which is valid if the instrumental line profile is a Gaussian line shape and the natural lifetime broadening effect corresponds to a Lorentzian. If the observed line profiles are fitted to Voigt functions $\Gamma$ as well as $k$ and $\tau$ can be derived through Eqs. (1) and (2).

In addition information on the intensities of rotationally resolved lines can provide *relative* predissociation rates, particularly in cases of accidental predissociation phenomena. In a previous study it was shown that in case of 1+1 ionization and under certain conditions the ion signal can be derived in a rate equation model resulting in[10]

$$I_{\rm ion} \propto N \frac{k_{\rm ion} k_{\rm abs}}{k_{\rm rad} + k_{\rm pred} + k_{\rm ion}}. \tag{3}$$

Here, $N$ is the population of the ground state and $k_{\rm abs}$, $k_{\rm rad}$, $k_{\rm pred}$, and $k_{\rm ion}$ are, respectively, the absorption rate for the bound–bound transition, the radiative decay rate of the intermediate state, the predissociation rate and the rate of ionization of the intermediate state. This relation holds under the condition of broadband excitation, i.e., the bandwidth of the light exceeds the natural width of the transition. Furthermore, the bound–bound transition should not be saturated. It is noted that $k_{\rm rad}$ and $k_{\rm pred}$ are molecular parameters and independent of laser intensities, while $k_{\rm abs}$ and $k_{\rm ion}$ are proportional to vuv and uv laser intensities, respectively. In case of 1 vuv+1 uv ionization both laser beams are completely defocused, and for a rapidly decaying state the ionization rate remains small ($k_{\rm ion} \ll k_{\rm pred}$) and can be considered constant, yielding[10]

$$I_{\rm ion} \propto N \frac{k_{\rm abs}}{k_{\rm rad} + k_{\rm pred}} \propto N k_{\rm abs} \tau. \tag{4}$$

Then the intensity along the rotational band is given by the product of Höhnl–London factor $k_{\rm abs}$ the Boltzmann population factor $N$ and the lifetime $\tau$ of the excited state. Any deviation from a smooth intensity behavior is the signature of a local perturbation.

Let us consider now a two-state model, where a rotational component $|s,J\rangle$ is perturbed by a state $|p,J\rangle$ with respective relaxation rates $\Gamma_s$ and $\Gamma_p$. Furthermore, a transition to state $|p\rangle$ is forbidden in excitation from the ground state. The mixing of $|s\rangle$ with $|p\rangle$ states diminishes the intensity by two effects. First, the intensity is proportional to the $s$ character of the mixed wave function $c_s^2$; thereby the transition to the $|p\rangle$ state receives oscillator strength as well. Second, the effective lifetime $\tau(J)$ or the relaxation rate $\Gamma(J)$ of the mixed state can be calculated from $\Gamma_s$ and $\Gamma_p$. Under these conditions a quantity $\eta$ may be defined which represents the effect of the perturbation on the intensity

$$\eta = \frac{c_s^2 \tau(J)}{\tau_s} = \frac{c_s^2 \Gamma_s}{\Gamma(J)}. \tag{5}$$

With this definition $\eta$ is the ratio of the actual intensity and the intensity if no perturbation by state $|p\rangle$ would occur.

Two final remarks must be made on the limitations of the model. First, Eqs. (3) and (4) are derived from a rate-equation model, and start to loose their validity when the laser bandwidth is comparable to the natural linewidth.[10] In the opposite regime of $\delta\nu_{\rm instr} \ll \Gamma$, where coherence effects come into play, the peak intensities are found to be proportional to $\tau^2$.[27] Second, in case of 2+1 REMPI processes the uv laser is focused to obtain a sufficiently high two-photon transition rate. Eq. (3) will still be valid for the ion yield

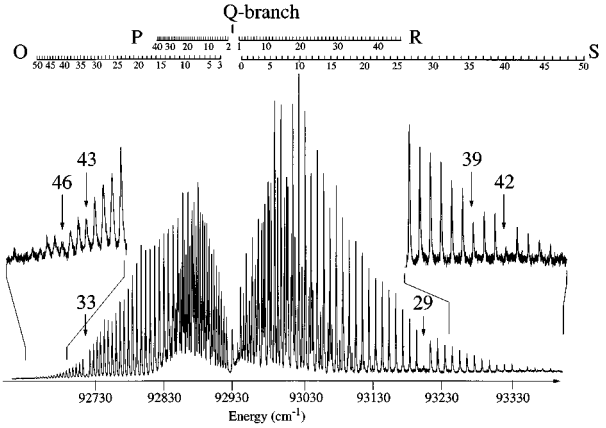


FIG. 2. Overview spectrum of the $E\ ^1\Pi - X\ ^1\Sigma^+$ (0,0) band recorded in natural CO with 2+1 REMPI. Because of the high temperature rotational states up to $J \approx 50$ are populated. The horizontal scale is obtained from calibration against the Tellurium standard and multiplication by four. Intensity effects at different lines probing $J_e = 31$, 41, and 44 states are indicated.

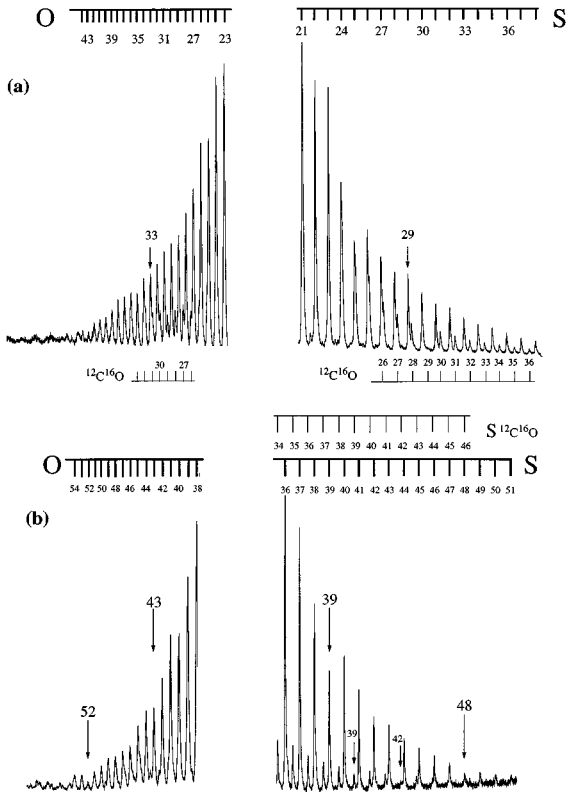


FIG. 3. Selected parts of the $E\ ^1\Pi - X\ ^1\Sigma^+$ (0,0) band recorded in enriched $^{13}C^{16}O$ with 2+1 REMPI spectroscopy. (a) and (b) cover corresponding parts of *O* and *S* branches. In (a) it is shown that $S(29)$ and $O(33)$ lines follow a regular intensity behavior, proving that $J_e = 31$ is not predissociated for $^{13}C^{16}O$. In (b) the newly observed predissociation phenomena are observable as intensity decreases of $S(39)$, $S(48)$ and corresponding $O(43)$ and $O(52)$ lines. The weak lines in the spectrum are due to $^{12}C^{16}O$ contamination.

provided $k_{abs}$ is taken as the two-photon absorption rate, which depends on the uv-intensity squared. Because of the focusing geometry with the high uv-intensities line strength as well as linewidth will depend on the ionization rate. The simplification of Eq. (4) is not allowed and there is not a simple quantitative relation for the relative intensities as a function of lifetime. However, in a qualitative sense locally observed intensity drops may be interpreted as accidental predissociations, although a simple proportionality with the lifetime $\tau$ is not available.

## IV. RESULTS

### A. 2+1 REMPI measurements

Figure 2 shows a typical 2+1 REMPI spectrum of the $E\ ^1\Pi - X\ ^1\Sigma^+(0,0)$ band recorded from a natural sample of CO. This transition is composed of five branches *O* ($\Delta J = -2$), *P* ($\Delta J = -1$), *Q* ($\Delta J = 0$), *R* ($\Delta J = 1$), and *S* ($\Delta J = 2$). The *P* and *R* branches probe *f*-parity $\Lambda$-doublet components of the $E\ ^1\Pi$ state, while the *e* states are probed in *O*, *S*, and *Q* branches. The high temperature of the sample allows thermal population of rotational ground states up to $J \approx 50$. The linewidth of each individual line is about 1 $cm^{-1}$ corresponding to the convolution of laser linewidth and the Doppler width (0.4 $cm^{-1}$ at 1000 K). Additional broadening effects were observed for pressures exceeding 4 Torr. All lines have been assigned and frequency calibrated with respect to the tellurium absorption spectrum and are included in a combined least squares minimization procedure with the data from the vuv excitation.

Interesting features are the anomalous intensity of some lines: The $O(33)$ and $S(29)$ lines have nearly completely disappeared, while the pairs $O(43)$, $S(39)$ and $O(46)$, $S(42)$ show an intensity reduced by a factor of 2 and 5, respectively. The corresponding parts of the spectrum are shown in the inset of Fig. 2. These perturbations are connected to the levels $J_e = 31$, 41, and 44. The accidental predissociation of $J_e = 31$ is well known but observed for the first time in a REMPI experiment. By enlarging the vertical scale a second spectral line could be distinguished 1.2 $cm^{-1}$ apart from the $S(29)$ line. The perturbations at $J_e = 41$ and 44 in the $E\ ^1\Pi$, $v = 0$ state of $^{12}C^{16}O$ were not observed before. The effect of intensity decrease is smaller than for $J_e = 31$ but nevertheless is clearly visible and reproduced in *O* and *S* branches.

Figures 3(a) and 3(b) show parts of the $E\ ^1\Pi - X\ ^1\Sigma^+(0,0)$ band registered for a sample enriched in $^{13}C$. The relative proportion of $^{13}C^{16}O$ and $^{12}C^{16}O$ is about 90/10. Weak lines in these spectra are easily attributed to $^{12}C^{16}O$. Figure 3(a) shows that the intensities of $S(29)$ and $O(33)$ lines follow an ordinary rotational line strength pattern, indicating that the accidental predissociation phenomenon at $E\ ^1\Pi$, $v = 0$, $J_e = 31$ does not exist for $^{13}C^{16}O$. In Fig. 3(b) the high *J* values of both *O* and *S* branches are shown. A weak but significant intensity decrease of $S(39)$ and $O(43)$ lines and a stronger effect on $S(48)$ and $O(52)$ appears. These results suggest that $E\ ^1\Pi$, $v = 0$, $J_e = 41$, and $J_e = 50$ states undergo accidental predissociation in $^{13}C^{16}O$.

The $E\ ^1\Pi - X\ ^1\Sigma^+(1,0)$ band has also been registered for both $^{13}C^{16}O$ and $^{12}C^{16}O$ reaching *J* values up to 43. The wavelength range for this band is unfortunately located at the high frequency limit of the tellurium absorption atlas,[22] so the *O* and *P* branches and only the beginning of the *R* and *S* branches could be calibrated using an interpolation proce-

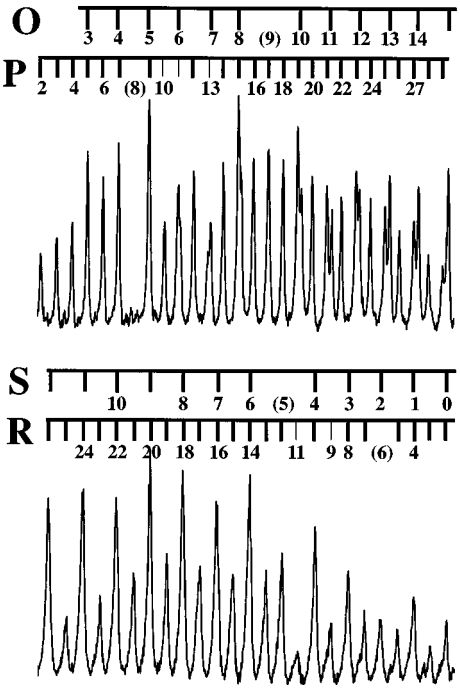


FIG. 4. Selected parts of the 2+1 REMPI spectrum of the $E\ ^1\Pi - X\ ^1\Sigma^+$ (1,0) band of $^{12}C^{16}O$ near the known perturbation at $J=7$. In the upper spectrum partly overlapping $O$ and $P$ branches are shown and in the lower spectrum $S$ and $R$ branches. The clearest feature showing predissociation is the vanishing of $P(8)$. Correspondingly the line at $R(6)$, which is overlapped by $S(2)$, lacks intensity. The distinct $R(9)$ and $R(11)$ lines are weakened and the same holds for the corresponding $P(11)$ and $P(13)$. The overlapped features $S(5)-R(12)$ and $O(9)-P(17)$ have lost intensity because of predissociation at $J_f=7$.

dure. No anomalous line intensities were observed for high $J$ values ($J>12$), indicating that accidental predissociation phenomena are absent. In Fig. 4 two parts of the 2+1 REMPI spectrum of $^{12}C^{16}O$ corresponding to low $J$ values are reproduced. Several irregularities are found: $P(8)$ is clearly missing, while $P(10)$, $P(11)$, and $P(13)$ have lower intensities than expected. The $O(9)$ line has nearly disappeared, i.e., the intensity at the frequency position of $O(9)$ is fully due to the overlapping $R(17)$ line. In the branches at the high energy side, shown in the lower part of Fig. 4, several intensity anomalies occur as well. First the overlapping feature $R(6)-S(2)$ is too weak. This can be ascribed to a missing $R(6)$ component, which similarly to $P(8)$ probes the $J_e=7$ level. The $R(9)$ and $R(11)$ lines are significantly weaker than expected from rotational line strengths. Similarly the overlapping $S(5)-R(12)$ feature lacks intensity. Combining this information leads to the conclusion that $J_f=7$, 9, 10, and 12 and $J_e=7$ levels of the $E\ ^1\Pi$, $v=1$ state of $^{12}C^{16}O$ are perturbed.

The 2+1 REMPI recording of the $E-X$ (1,0) band of $^{13}C^{16}O$ is similar to that of the $^{12}C^{16}O$ isotope. Near the low $J$ values again the $P(8)$ line is missing, while the overlapping $S(5)-R(12)$ and $S(2)-R(6)$ features are too weak. Similarly, the $P(11)-O(6)$ feature is weak with respect to neighboring lines. In contrast to $^{12}C^{16}O$ the $P(13)$ line has not lost any intensity in $^{13}C^{16}O$. From the REMPI spectra it is concluded that $J_e=J_f=7$ and possibly $J_f=10$ predissociate.

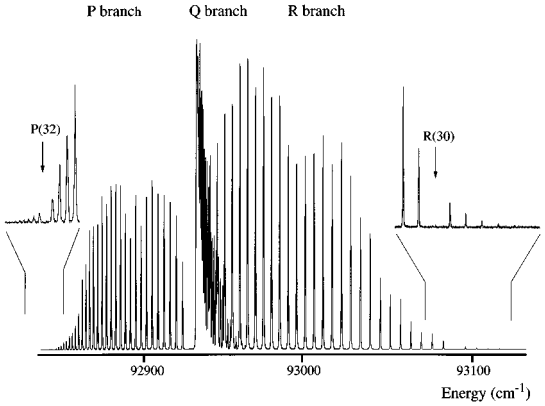


FIG. 5. Overview spectrum of the $E\ ^1\Pi - X\ ^1\Sigma^+$ (0,0) band recorded with 1 vuv+1 uv photoionization in a molecular beam. High $J$ lines in the $Q$ branch are clearly resolved for the first time. In the insets the vanishing of $R(30)$ and $P(32)$ lines, due to the well known accidental predissociation at $J_e=31$ is displayed.

### B. Vuv measurements

Excitation with narrowband vacuum ultraviolet radiation was performed in a molecular beam expansion of carbon monoxide. As large quantities of CO are required for the production of a molecular beam only samples of natural CO could be used. However, the combination of high sensitivity in the ion detection system with the mass separation by time

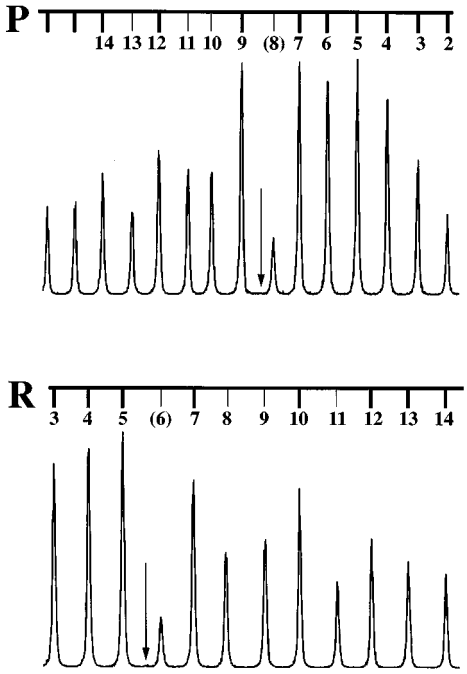


FIG. 6. Selected parts of the vuv spectrum of the $E\ ^1\Pi - X\ ^1\Sigma^+$ (1,0) band of $^{12}C^{16}O$ near the known perturbation at $J_e=7$. In the upper spectrum the relative intensity decrease in $P(8)$, $P(10)$, $P(11)$, and $P(13)$ is clearly visible. Similarly in the lower spectrum the corresponding $R(6)$, $R(8)$, $R(9)$, and $R(11)$ have lost relative intensity. An additional barely visible feature, a transition to the $k\ ^3\Pi_0$, $v=5$, $J_e=7$ perturber state, is marked by an arrow.

of flight after ionization enables us to record spectra of other isotopes than $^{12}C^{16}O$. At mass 29, selected with an appropriate gate of the boxcar integrator, overlapping spectra of $^{13}C^{16}O$ and $^{12}C^{17}O$ were obtained, while at mass 30 a spectrum of $^{12}C^{18}O$ was recorded. All spectra for the various isotopomers were obtained in simultaneous laser scans. Unfortunately the mass separation is not perfect, particularly at wavelength positions where intense $^{12}C^{16}O$ features are excited. Therefore, the spectra of minority species are contaminated. An example of an excitation spectrum of the $E\ ^1\Pi$, $v=0$ state of $^{12}C^{16}O$, recorded by 1 vuv+1 uv photoionisation near $\lambda=107$ nm, is shown in Fig. 5. Beam conditions were optimized for the highest rotational temperature ($T=270\pm10$ K) so that rotational progressions could be followed up to $J=35$. Unfortunately, the new predissociations at $J_e=41$, 44, and 50 in the two-photon spectra could not be reconfirmed in the vuv-excitation studies, because of the relatively low temperature. The accidental predissociation phenomenon at $J_e=31$ is clearly visible in the insets of Fig. 5: the $R(30)$ and $P(32)$ lines have completely disappeared.

In Fig. 6 spectra of the $P$ and $R$ branches excited near the $E\ ^1\Pi$, $v=1$, $J_e=7$ state of $^{12}C^{16}O$ are displayed. Again the intensities of $P(8)$ and $R(6)$ lines are too low because of predissociation, but the lines have not totally disappeared. In both cases a second weak component is observed, similar as in previous studies.[4,7,11] Both $R(11)$ and $P(13)$ lines probing $J_e=12$ are weakened. Similarly $P(10)$ and $P(11)$ and the corresponding $R(8)$ and $R(9)$ lines are weaker than expected. These phenomena are all attributed to accidental predissociation (see below). In the 1 vuv+1 uv ionization spectra of $^{13}C^{16}O$, shown in Fig. 7, the $P(8)$ and $R(6)$ lines have disappeared. A further example of predissociation is found in the relative weakening of $P(11)$. An intensity analysis of the spectral feature of $R(9)$, which is partly overlapped by a $^{12}C^{16}O$ components yields the same result.

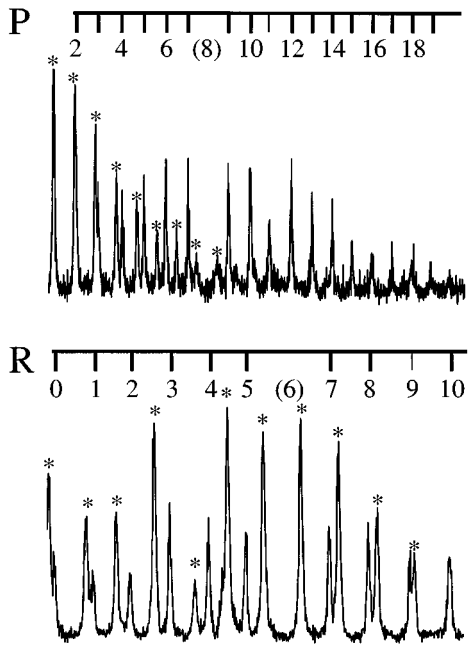


FIG. 7. Selected parts of the vuv spectrum of the $E\ ^1\Pi-X\ ^1\Sigma^+$ (1,0) band of $^{13}C^{16}O$ near the known perturbation at $J_e=7$. Because these spectra were recorded in natural abundance contaminations from $^{12}C^{16}O$ are present and marked by (*). In the upper spectrum the $P(8)$ line has completely vanished, while in the lower spectrum the $R(6)$ line has disappeared. In the $P$ branch the weakening of $P(11)$ is apparent, while from a deconvolution of the overlapping $^{12}C^{16}O$ line at $R(9)$ the same follows.

### C. Spectroscopic results

The 2+1 REMPI spectra obtained from a hot CO sample with rotational state population up to $J\approx50$ as well as 1 vuv+1 uv photoionization spectra in a molecular beam were carefully recorded for transitions to the $E\ ^1\Pi$, $v=0$ and $v=1$ states. The lines in the vuv spectrum were symmetric and narrow (0.4 $cm^{-1}$) and for the main isotope an internal consistency of 0.04 $cm^{-1}$ in the frequency positions was found. Spectra of the minor isotopic species were recorded from natural samples of CO (1% $^{13}C^{16}O$, 0.2% $^{12}C^{18}O$, 0.04% $^{12}C^{17}O$) and therefore signal-to-noise ratios are smaller, determination of line position less accurate and fewer lines recorded. In the 2+1 REMPI spectra the observed linewidths were 1 $cm^{-1}$, while line shapes were asymmetric as a result of ac–Stark broadening in the focal region. Therefore the derived transition frequencies are less

TABLE I. Molecular constants for the $E\ ^1\Pi$, $v=0$ and $v=1$ states of $^{12}C^{16}O$. All values in $cm^{-1}$.

| | | This work | Ref. 16 | Ref. 11 | Ref. 21 |
|---|---|---|---|---|---|
| $v=0$ | $T_0$ | 92 929.912 (8) | 92 929.97 (4) | 92 929.95 (5) | |
| | $B_e$ | 1.964 62 (3) | 1.964 61 (1) | | 1.964 50 (24) |
| | $B_f$ | 1.952 62 (5) | 1.952 69 (1) | 1.952 82 (16) | 1.952 64 (14) |
| | $q$ | 0.011 82 (3) | 0.011 92 (1) | 0.011 87 (13) | 0.011 86 (10) |
| | $D_e$ | 6.547 (14) $10^{-6}$ | 6.54 (2) $10^{-6}$ | 6.5 (1) $10^{-6}$ [a] | 6.0 (3) $10^{-6}$ [a] |
| | $D_f$ | 6.29 (5) $10^{-6}$ | 6.36 (2) $10^{-6}$ | | |
| | $q_D$ | 0.25 (5) $10^{-6}$ | 0.18 (3) $10^{-6}$ | | |
| $v=1$ | $T_1$ | 95 082.881 (13) | | 95 082.90 (5) | |
| | $B_e$ | 1.939 68 (5) | | | |
| | $B_f$ | 1.928 23 (7) | | 1.928 1 (4) | |
| | $q$ | 0.011 45 (9) | | 0.011 5 (3) | |
| | $D_e$ | 7.05 (4) $10^{-6}$ | | | |
| | $D_f$ | 6.92 (6) | | 7.1 (1) $10^{-6}$ | |
| | $q_D$ | 0.13 $10^{-6}$ | | | |

[a]Only a single $D$ constant used in fit.

TABLE II. Molecular constants for the $E\ ^1\Pi$, $v=0$ and $v=1$ states of $^{13}C^{16}O$. All values in $cm^{-1}$.

| | | This work | Ref. 11 | Ref. 29 |
|---|---|---|---|---|
| $v=0$ | $T_0$ | 92 929.709 (8) | 92 929.81 (17) | |
| | $B_e$ | 1.877 82 (3) | | |
| | $B_f$ | 1.866 90 (7) | 1.867 00 (12) | 1.866 4 (2) |
| | $q$ | 0.010 92 (9) | 0.010 83 (10) | 0.011 2 (3) |
| | $D$ | 6.004 (13) $10^{-6}$ | 6.1 (1) $10^{-6}$ | |
| $v=1$ | $T_1$ | 95 035.92 (2) | 95 035.94 (5) | |
| | $B_e$ | 1.854 92 (8) | | |
| | $B_f$ | 1.844 24 (8) | 1.844 36 (14) | |
| | $q$ | 0.010 68 (11) | 0.010 66 (10) | |
| | $D$ | 6.50 (8) $10^{-6}$ | 6.6 (2) $10^{-6}$ | |

accurate and somewhat shifted from the true position. The recording of high $J$-components, however, yields valuable information for a determination of molecular parameters.

For transitions to $E\ ^1\Pi$, $v=0$ and $v=1$ states of $^{12}C^{16}O$ a total number of 225 and 160 transition frequencies were recorded in different branches of the one and two photon spectra. For the $E\ ^1\Pi$, $v=0$ state of $^{12}C^{16}O$ the resolution in combination with the sensitivity was high enough to record for the first time $Q$-branch lines up to $Q(27)$. Results of multiple measurements of each line are averaged and errors properly weighted. On average the unblended lines from the REMPI spectra are downweighted in the fit by a factor of 2 with respect to the lines in the vuv spectra. It is noted that the main error in the transition frequency of the CO lines originates from the determination of the line positions in the calibration spectra, i.e., 0.04 $cm^{-1}$ for $I_2$ and 0.06 $cm^{-1}$ for $Te_2$. For $^{13}C^{16}O$ the total number of data included in the fit was 190 for $v=0$ and 130 for $v=1$. A limited number of frequency positions for the $E\ ^1\Pi$, $v=0$ and $v=1$ states of $^{12}C^{18}O$ and $^{12}C^{17}O$ was derived from the vuv spectra only. For the sake of brevity the lengthy tables of transition frequencies are not presented here, but are available upon request. The data obtained in one- and two-photon spectra for a certain state and isotope were combined in a single least-squares minimization routine. The energies of the $X\ ^1\Sigma^+$ ground state levels were calculated from the constants of Guelachvili *et al.*[28] The outcome of these fitting procedures is presented in Tables I–IV for the four different isotopomers observed. The lines that were found to be affected by local

TABLE III. Molecular constants for the $E\ ^1\Pi$, $v=0$ and 1 states of $^{12}C^{18}O$. All values in $cm^{-1}$.

| | | This work | Ref. 11 | Ref. 30 |
|---|---|---|---|---|
| $v=0$ | $T_0$ | 92 929.51 (2) | 92 929.74 (5) | |
| | $B_e$ | 1.8703 (1) | | |
| | $B_f$ | | 1.859 64 (14) | 1.859 74 (18) |
| | $q$ | | 0.010 62 (10) | 0.011 07 (17) |
| | $D$ | 5.6 (1) $10^{-6}$ | 6.6 (2) $10^{-6}$ | |
| $v=1$ | $T_1$ | 95 031.86 (3) | 95 031.92 (5) | |
| | $B_e$ | 1.8487 (5) | | |
| | $B_f$ | | 1.837 4 (2) | |
| | $q$ | | 0.010 3 (2) | |
| | $D$ | 6.0 $10^{-6}$ [a] | 6.2 (3) $10^{-6}$ | |

[a]Fixed in fit.

TABLE IV. Molecular constants for the $E\ ^1\Pi$, $v=0$ state of $^{12}C^{17}O$. Values in $cm^{-1}$.

| | |
|---|---|
| $T_0$ | 92 929.67 (4) |
| $B_e$ | 1.9146 (3) |
| $D$ | 5.9 (4) $10^{-6}$ |

perturbations, resulting in line shifts, were omitted from the fits. Because the 2+1 REMPI lines were somewhat asymmetric the band origin for these lines was independently varied. From all fitting routines an offset of $0.20\pm0.05$ $cm^{-1}$, due to this asymmetry, could be deduced. The true band origin, as given in Tables I–IV is determined from the narrow vuv lines. We note here that the recalibration of the $I_2$ standard[24] is accounted for. The accuracy of the constants pertaining to the $e$-parity components is better, because a larger number of transitions was observed than for $f$ components (observed in $P$ and $R$ branches in two photon excitation and the $Q$ branch in one-photon excitation). The constants with subscripts $e$ and $f$ refer to the parity components, where the rotational constant $B_e$ should not be confused with the equilibrium value $B_e$ [see below, Eq. (7)]. For $^{12}C^{18}O$ only $e$ states could be probed, up to $J_e=28$ for $v=0$ and $J_e=12$ for $v=1$. Also for $^{12}C^{17}O$ only $e$ states of $E\ ^1\Pi$, $v=0$ were probed for $J$ in between 9 and 20. The data on the main $^{12}C^{16}O$ isotope were accurate enough to even determine a centrifugal distortion effect on the $\Lambda$ doubling, or correspondingly different values for centrifugal distortion constants $D_e$ and $D_f$.

### D. Data on accidental predissociations

Accidental predissociation phenomena were uncovered from the spectra by monitoring intensity irregularities (see Sec. III) and by accurate determination of line shifts. Extra checks are possible as observed effects should be reproduced in spectral components probing the same excited levels, such as the combination of $S(J-2)$ and $O(J+2)$ lines. From the intensity analysis of 2+1 REMPI data for $^{12}C^{16}O$ we found that $E\ ^1\Pi$, $v=1$, $J_f=7$, 9, 10, 12 undergo accidental predissociation, while particularly the vuv data showed that $J_e=7$, 9, 10, 12 are perturbed. For $^{13}C^{16}O$ accidental predissociations are most decisive at $J_f=J_e=7$ and $J_f=J_e=10$. As far as the $E\ ^1\Pi$, $v=0$ state is concerned perturbations are only found for $e$-parity components. For $^{12}C^{16}O$ $J_e=31$, 41 and 44 are perturbed while in $^{13}C^{16}O$ this holds for $J_e=41$ and 50. Spectral data, such as frequency positions and relative intensity for all lines related to local perturbations of the $E\ ^1\Pi$, $v=0$ state of $^{12}C^{16}O$ are given in Table V. For $J_e=31$ we could derive values for the intensity ratio $\eta$ from the $R$ branch of the $E-X$ (0,0) band in the vuv spectrum. From the 2+1 REMPI spectra significantly lower values of $\eta$ were found, as expected in case of ionization saturation (see Sec. III).

For the $E\ ^1\Pi$, $v=1$, $J_e=7$ level of $^{12}C^{16}O$ the vuv spectra gave valuable information. First a transition to the perturber state, known as the $k\ ^3\Pi_0$, $v=5$, $J_e=7$ level,[17] was observed as a very weak extra line at 95 104.24 $cm^{-1}$ with

TABLE V. Spectral data on predissociation, $e$ parity and high $J$ values in the $E\ ^1\Pi$, $v=0$ state of $^{12}C^{16}O$. $\Delta$ represents the difference between the experimental energy and the calculated term value from molecular constants. $\eta$ is the observed intensity decrease (see the text) as obtained from 2+1 REMPI experiments. The values denoted by $31_k$ pertain to the $k\ ^3\Pi_2$, $v=3$, $J_e=31$ state, whereas the state denoted by 31 refers to the $E\ ^1\Pi$, $v=0$, $J_e=31$ state; it is noted that these two states are strongly mixed and the $k$-state component could be observed through intensity borrowing from the $E$ state. The weaker component is then assigned as the state with dominant $k$-state character.

| $J$ value | Exp. Energies ($cm^{-1}$) | Calculated term values ($cm^{-1}$) | $\Delta$ ($cm^{-1}$) | $\eta$ |
|---|---|---|---|---|
| $31_k$ | 94 871.59 (15) | 94 872.397 | −0.807 | 0.07 |
| 31 | 94 872.87 (08) | 94 872.347 | 0.523 | 0.12 |
| 41 | 96 293.51 (09) | 96 293.581 | −0.07 | 0.71 |
| 44 | 96 794.02 (06) | 96 794.202 | −0.186 | 0.35 |

TABLE VI. Experimental data pertaining to the interaction between $E\ ^1\Pi$, $v=1$ and $k\ ^3\Pi$, $v=5$ $e$-parity states of $^{12}C^{16}O$ in the range $J=5-13$ as obtained from the vuv spectra. $\Delta_{exp}$ represents the difference between experimental term values and energies obtained with constants of Table I. $\eta_{exp}$ represents the experimental intensity factor (see the text).

| $J$ | Exp. energy ($cm^{-1}$) | $\Delta_{exp}$ ($cm^{-1}$) | $\eta_{exp}$ |
|---|---|---|---|
| 5 | 95 141.005 | −0.060 | 0.95 |
| 6 | 95 164.258 | −0.077 | 0.93 |
| $7_k$ | 95 190.057 | | 0.007 |
| 7 | 95 191.790 | +0.309 | 0.24 |
| 8 | 95 222.464 | −0.038 | 0.89 |
| 9 | 95 257.114 | −0.281 | 0.60 |
| 10 | 95 296.383 | +0.222 | 0.70 |
| 11 | 95 338.864 | +0.068 | 0.86 |
| 12 | 95 385.516 | +0.216 | 0.59 |
| 13 | 95 435.678 | +0.009 | 0.96 |

an intensity of 2.5% of that of the $R(6)$ line of the $E-X$ (1,0) band. Moreover, for the first time predissociation-induced line broadening could be observed for these lines. The $R(6)$ and $P(8)$ lines in the vuv spectra have an average width of $0.49\pm0.03$ $cm^{-1}$ and are found to be significantly and reproducibly broader than other lines that have widths in the range 0.37–0.43 $cm^{-1}$. The very weak transition to the $k\ ^3\Pi_0$, $v=5$, $J_e=7$ perturber was also observed as a broadened feature, but its intensity is too weak to derive a trustworthy value.

In the work of Amiot *et al.*[16] a local perturbation was found in $^{12}C^{16}O$ at $E\ ^1\Pi$, $v=0$, $J_f=6$ as an intensity decrease in the $E\ ^1\Pi-B\ ^1\Sigma^+$ emission spectrum. Inspection of our 2+1 REMPI spectra did not reveal significant intensity effects on $P(7)$ and $R(5)$ lines probing this $J_f=6$ level. Mellinger and Vidal[19] have explained this perturbation by the presence of the $j\ ^3\Sigma^+$ state and furthermore suggested that predissociation effects could occur near $E\ ^1\Pi$, $v=0$, $J_f=36$, and $J_e=15$ levels. In both 2+1 REMPI and vuv spectra we have found no evidence of line shifts or intensity decreases at $J_e=15$. The $R(35)$ component was overlapped with a strong $S$ branch feature prohibiting a conclusion concerning $J_f=36$.

In Table VI we have compiled data pertaining to an analysis of line shifts and relative intensities near accidental predissociations. Transition frequencies of these lines were not used to derive molecular constants.

## V. ANALYSIS OF THE PREDISSOCIATION PHENOMENA

In a recent study Baker *et al.*[11] interpreted the perturbations at $E\ ^1\Pi$, $v=0$, $J_e=31$ and $E\ ^1\Pi$, $v=1$, $J_e=7$ in terms of a crossing with a triplet state $k\ ^3\Pi$ state, with vibrational levels $v=3$ and 5, respectively. Later more accurate information on the $k\ ^3\Pi$ state became available through the recording of $k\ ^3\Pi-X\ ^1\Sigma^+(v,0)$ absorption bands for $v=2$, 3, and 5[17] and more recently for $v=0$.[20] Following the graphical analysis of Baker and Launay, we constructed energy vs $J(J+1)$ diagrams (cf. reduced term value plots as in Figs. 5 and 6 of Ref. 17) for $E\ ^1\Pi$, $v=0$ and $v=1$ states and $k\ ^3\Pi$, $v$ perturber states. The $v=4$ component of this $k\ ^3\Pi$ state seems to be a good candidate to explain the $J_e=41$ and 44 perturbations presently observed. Molecular parameters for $k\ ^3\Pi$ $v=4$ were determined from the following relations:

$$T_v=T_e+\omega_e\left(v+\frac{1}{2}\right)+\omega_e x_e\left(v+\frac{1}{2}\right)^2 \tag{6}$$

and

$$B_v=B_e-\alpha_e\left(v+\frac{1}{2}\right) \tag{7}$$

and by fitting these to the known molecular constants for $k\ ^3\Pi$, $v=2$, 3, and 5.[17] This procedure yields $T_e=91\ 803.5$ $cm^{-1}$, $\omega_e=838.9$ $cm^{-1}$, $\omega_e x_e=5.8$ $cm^{-1}$, $B_e=1.3204$ $cm^{-1}$, $\alpha_e=0.028\ 35$ $cm^{-1}$, and slightly different when $v=0$[20] is included. Note that $T_e$ of the excited states is as usual taken with respect to the potential minimum of the $X\ ^1\Sigma^+$ ground state and includes a zero-point vibrational energy of 1081.6 $cm^{-1}$. For $v=4$ Eqs. (6) and (7) give: $T_4=94379.5$ $cm^{-1}$ and $B_4=1.19$ $cm^{-1}$. Here, we have followed the convention of defining $T_v$ with respect to $X\ ^1\Sigma^+$, $v=0$, $J=0$. In the following analysis the spin-coupling, $\Lambda$-doubling, and centrifugal distortion constants are kept fixed: $A=31$ $cm^{-1}$, $\lambda=0$ $cm^{-1}$, $o+p+q=0.298$ $cm^{-1}$, $D=1.0\times10^{-5}$ $cm^{-1}$. For $k\ ^3\Pi$, $v=1$ the derived constants yield $T_1=91\ 967.17$ $cm^{-1}$ which deviates by 8 $cm^{-1}$ from the accurate value of 91 959.354 (24) $cm^{-1}$, reported recently by Mellinger and Vidal.[19] This shift is consistent with the observation of the vibrational series $v=0,1,2,3$ of the state now identified as $k\ ^3\Pi$ by Wan and Langhoff,[18] who have pointed out that a perturbation exist at $v=1$, which pushes down the level by 9 $cm^{-1}$.

Based on the constants derived and using the effective Hamiltonian for a $^3\Pi$ state[31] the energy levels of $^3\Pi_\Omega(J)$ $e$-parity components were calculated for the $k\ ^3\Pi$, $v=4$ state. In Fig. 8 these energies and those of $k\ ^3\Pi$, $v=3$ and 5 and $E\ ^1\Pi$, $v=0$ states for $^{12}C^{16}O$ are presented in a reduced term value plot. Crossing points, corresponding to local perturbations, are indicated with circles. The perturbation of $E\ ^1\Pi$, $v=0$, and $k\ ^3\Pi_{2e}$, $v=3$ at $J_e=31$ was discussed in a similar treatment by Baker and Launay.[17] Two additional quasi-coincidences are found between $E\ ^1\Pi$, $v=0$ with

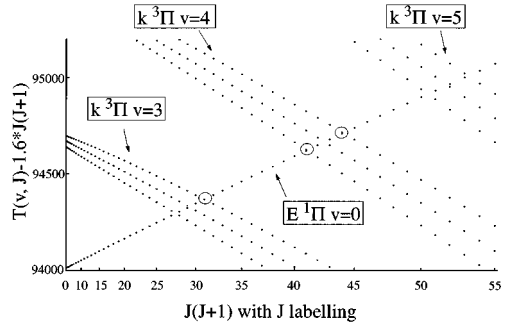


FIG. 8. Calculated term values for $k\ ^3\Pi$, $v=3$, 4, and 5 and $E\ ^1\Pi$, $v=0$ $(e)$-parity levels of $^{12}C^{16}O$ as a function of $J(J+1)$. For clarity a value of $1.6*J(J+1)$ is subtracted. Circles indicate the near coincidences that cause accidental predissociations. Term values are given with respect to the bottom of the $X\ ^1\Sigma^+$ ground state potential well and include a zero-point energy of 1081.6 $cm^{-1}$.

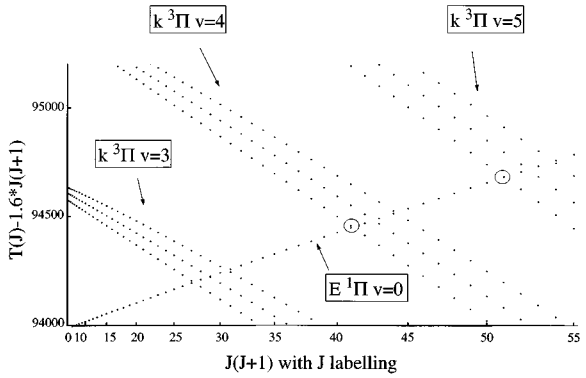


FIG. 9. Calculated term values for $k\ ^3\Pi$, $v=3$, 4, and 5 and $E\ ^1\Pi$, $v=0$ $(e)$-parity levels of $^{13}C^{16}O$ as a function of $J(J+1)$. Circles indicate the near coincidences that cause accidental predissociations. Term values are given with respect to the bottom of the $X\ ^1\Sigma^+$ ground state potential well and include a zero-point energy of 1057.5 $cm^{-1}$.

$k\ ^3\Pi_{0e}$, $v=4$ and $k\ ^3\Pi_{2e}$, $v=4$ occuring, respectively, at $J_e=41$ and 44. The calculated energy differences at these crossings are 2 and 3 $cm^{-1}$. Although the calculated $k$-state energies are not expected to be extremely accurate, the procedure using interpolated molecular constants provides a convincing explanation for the newly observed predissociation phenomena in $E\ ^1\Pi$, $v=0$, $J_e=41$ and 44 levels.

The diagram in Fig. 8, extended to values up to $J\approx 55$, shows that the next crossing of the $E\ ^1\Pi$, $v=0$ with the $k\ ^3\Pi$, $v=5$ state occurs in the range $J_e=50-54$. For the $^{12}C^{16}O$ isotope the rotational manifold could not be recorded up to such high $J$, but for $^{13}C^{16}O$ this was possible. The reduced term value plot suggests that the perturbations observed for $^{13}C^{16}O$ can be explained in the same way. However no spectroscopic data have been reported on the $k\ ^3\Pi$ state of $^{13}C^{16}O$. Therefore, we used isotopic scaling to determine the spectroscopic constants[25]

$$T_e^i=T_e,\quad \omega_e^i=\omega_e\rho,\quad \omega_e x_e^i=\omega_e x_e\rho^2,$$
$$B_e^i=B_e\rho^2,\quad D_e^i=D_e\rho^4,\quad \alpha_e^i=\alpha_e\rho^3, \tag{9}$$

where the indexed constants relate to $^{13}C^{16}O$ and $\rho$ is

$$\rho=\sqrt{\frac{\mu}{\mu_i}} \tag{10}$$

with $\mu$ and $\mu_i$ are the reduced masses of the isotopomers. For the $k\ ^3\Pi$ state of $^{13}C^{16}O$ this yields $T_e=90\ 746.01$ $cm^{-1}$, $\omega_e=820.24$ $cm^{-1}$, $\omega_e x_e=5.58$ $cm^{-1}$, $B_e=1.260$ $cm^{-1}$, $\alpha_e=0.0265$ $cm^{-1}$, $D=9\times10^{-6}$ $cm^{-1}$. The zero-point energy for the $X\ ^1\Sigma^+$ ground state of $^{13}C^{16}O$ is 1057.5 $cm^{-1}$. For the spin-coupling and $\Lambda$-doubling constants the same values as for $^{12}C^{16}O$ were assumed. Using thus obtained molecular constants the energies of $k\ ^3\Pi_\Omega$, $v=3$, 4, and 5 levels were calculated for the $e$-parity components of various $J$ states. Next a reduced term value plot for $^{13}C^{16}O$ was constructed, which is shown in Fig. 9. Crossings are found in approximately the same $J$ regions as in $^{12}C^{16}O$: 27–31, 41–44, and 51–54. Based on these calculations perturbations are expected at $J_e=27$ and 29 for the crossing with $k\ ^3\Pi$, $v=3$, at $J_e=41$ and 44 for the crossing with $k\ ^3\Pi$, $v=4$ and at $J_e=51$ for the crossing with $k\ ^3\Pi$, $v=5$. Experimentally for $^{13}C^{16}O$ no perturbation appeared at $J_e=31$ in agreement with the diagram. Also no effect of a perturbation is visible near the expected crossings $J_e=27$ or 29. A weak perturbation is observed at $J_e=41$ in agreement with the prediction of a perturbation by the $^3\Pi_0$ component. The perturbation observed at $J_e=50$ disagrees with the calculation, where a crossing is found at $J_e=51$. The model using the isotopic scaling and extrapolation to high $J$ values obviously is not sufficiently accurate. The observed perturbations suggests that the $k\ ^3\Pi$ energies should be slightly lower than calculated. Although the calculation of the perturber state is off by one rotational quantum, the origin of the accidental predissociation of the $E\ ^1\Pi$, $v=0$, $J_e=50$ state is clearly identified.

An explanation for the origin of the perturbations near $E\ ^1\Pi$, $v=1$, $J=7$ of $^{12}C^{16}O$ was given by Baker and Launay.[17] At $J=7$ the energy of $E\ ^1\Pi$, $v=1$ and $k\ ^3\Pi_0$, $v=5$ are in near coincidence: 0.07 $cm^{-1}$ energy difference for $J_f=7$ and 1.7 $cm^{-1}$ for $J_e=7$. This might explain why the $P(8)$ line, probing the $J_f=7$ level, in our 2+1 REMPI spectrum has completely vanished, while the transitions probing the $J_e=7$ level have lost only part of their intensity. The $k\ ^3\Pi_2$ state was found to cross at $J=12$ (detunings of 4.3 $cm^{-1}$ for $e$ and 1.9 $cm^{-1}$ for $f$). Indeed, we found a weak but distinctive predissociation effect on both $J_e=12$ and $J_f=12$. The $k\ ^3\Pi_1$ triplet component crosses in between $J=9$ and 10 with larger detunings for both $e$ and $f$ components (cf. Fig. 6 of Ref. 17). This already explains in a qualitative sense the observed predissociation phenomena in our vuv and 2+1 REMPI spectra.

For a quantitative analysis of these perturbations we consider primarily the more accurate data of the vuv spectra. Lines corresponding to $J_e=7$, 9, 10, 12 are found to be shifted and have lower intensities than expected. In Table VI the experimental data for the states $J_e=5$ to 13 are summarized. The term values for $E\ ^1\Pi$, $v=1$, $J_e$ states are deduced by averaging results from $P$ and $R$ branch lines. Perturbative shifts $\Delta_{\rm exp}(J_e)$ represent the difference between these experimental term values and the energy values calculated with the molecular constants of Table I. A quantitative analysis of the

TABLE VII. Values for term energies, perturbative shifts $\Delta_{calc}$, singlet character of the wave function $c_E^2$, decay rate $\Gamma$, and intensity factor $\eta_{calc}$, calculated from matrix diagonalization at the interaction between $E\ ^1\Pi$, $v=1$ and $k\ ^3\Pi$, $v=5$ states in the range $J=5-13$. In the last column $J$-dependent lifetimes are given for $e$-parity components of the $E\ ^1\Pi$, $v=1$ state.

| $J$ | Term energy ($cm^{-1}$) | $\Delta_{calc}$ ($cm^{-1}$) | $c_E^2$ | $\Gamma$ ($cm^{-1}$) | $\eta_{calc}$ | $\tau$ ($10^{-10}$s) |
|---|---|---|---|---|---|---|
| 5 | 95 140.986 | −0.079 | 0.9982 | 0.054 | 0.977 | 0.98 |
| 6 | 95 164.226 | −0.106 | 0.9953 | 0.056 | 0.942 | 0.95 |
| $7_k$ | 95 190.051 | −0.347 | 0.2057 | 0.569 | 0.019 | 0.093 |
| 7 | 95 191.734 | +0.250 | 0.7915 | 0.185 | 0.228 | 0.29 |
| 8 | 95 222.402 | −0.098 | 0.9915 | 0.058 | 0.898 | 0.91 |
| 9 | 95 257.083 | −0.313 | 0.9613 | 0.078 | 0.653 | 0.68 |
| 10 | 95 296.433 | +0.273 | 0.9646 | 0.076 | 0.674 | 0.70 |
| 11 | 95 338.822 | +0.025 | 0.9909 | 0.059 | 0.892 | 0.90 |
| 12 | 95 385.621 | +0.322 | 0.9367 | 0.094 | 0.530 | 0.57 |
| 13 | 95 435.758 | +0.089 | 0.9972 | 0.055 | 0.964 | 0.97 |

observed line intensities in $P$ and $R$ branches was performed, using calculated Höhnl–London and Boltzmann population factors. This procedure yields a rotational temperature of $270\pm10$ K and values for $\eta_{exp}$, the intensity ratio factor. Results for $\eta_{exp}$ are listed in Table VI.

A model for this interaction is based on a spin-orbit coupling $H^{SO}$ between $^1\Pi$ and $^3\Pi$ states. This coupling can be reduced to a sum of monoelectronic terms over all the electrons

$$H^{SO}=\sum_i a_i(\mathbf{l}_i\cdot\mathbf{s}_i)=\sum_i a_i\left[l_{iz}s_{iz}+\frac{1}{2}(l_i^+s_i^-+l_i^-s_i^+)\right]. \quad (11)$$

Following Lefebvre-Brion and Field[32] selection rules apply for this perturbation between states that differ by zero or one single electron orbital; in all cases $\Delta\Omega=0$, $\Delta S=0,\pm1$, $\Delta J=0$, and $e/f$ parity conservation hold. For the first term involving $a_i l_{iz}s_{iz}$ furthermore $\Delta\Lambda=\Delta\Sigma=0$ applies, while for the other term in Eq. (11) $\Delta\Lambda=-\Delta\Sigma=\pm1$ applies. Apparently, only the first term $a_i l_{iz}s_{iz}$ gives rise to a coupling between $\Pi$ states. These selection rules indicate that $E\ ^1\Pi_1$ state can only couple with the $^3\Pi_1$ component of the $k$ state. For a perturbation analysis a matrix of the form

$$\begin{pmatrix} E\ ^1\Pi & 0 & V^{SO} & 0 \\ 0 & k_{22} & k_{12} & k_{02} \\ V^{SO} & k_{21} & k_{11} & k_{01} \\ 0 & k_{20} & k_{10} & k_{00} \end{pmatrix} \quad (12)$$

must be diagonalized for each value of $J$, where the submatrix $k_{ij}$ of $k\ ^3\Pi$ on a basis $\{^3\Pi_2,^3\Pi_1,^3\Pi_0\}$ is taken from Brown and Merer.[31] The subscripts $i$ and $j$ refer to the values of $\Omega$ and only $e$-parity levels are considered here. Molecular constants for $k\ ^3\Pi$, $v=5$ were taken from Baker and Launay[17] and for $E\ ^1\Pi$, $v=1$ from Table I. $V^{SO}$ is the only nonzero $J$-independent off-diagonal element between $E$ and $k$ subspace

$$V^{SO}=\left\langle k\ ^3\Pi_{1e}\left|\sum_i a_i\mathbf{l}_i\cdot\mathbf{s}_i\right|E\ ^1\Pi_{1e}\right\rangle\langle\nu_k|\nu_E\rangle, \quad (13)$$

where the last factor is the Franck–Condon overlap between vibrational wave functions of $E\ ^1\Pi$ and $k\ ^3\Pi$ states. First line shifts were analyzed. Term values were calculated for $V^{SO}=0$ and different values of $V^{SO}$. Differences in term values $\Delta_{calc}$ obtained from these calculations are presented in Table VII for $V^{SO}=2.0\ cm^{-1}$, which gave the best agreement with the experimental data. A comparison between $\Delta_{calc}$ and $\Delta_{exp}$ is given in Fig. 10. The agreement is good and confirms the assumption of the perturbation as a spin-orbit coupling.

With the value for the parameter $V^{SO}=2.0\ cm^{-1}$ the effects of intensity changes near the perturbation are considered next. Recalling the assumption of Eq. (4), that the intensities are proportional to the lifetime we performed the matrix diagonalization by adding an imaginary part $-i\Gamma_E/2$ or $-i\Gamma_k/2$ to the diagonal elements in the matrix of Eq. (13). Here, we extend procedures established by Cohen-Tannoudji *et al.*[33] for the case of interaction between a bound state and a decaying state, to the case of four decaying states

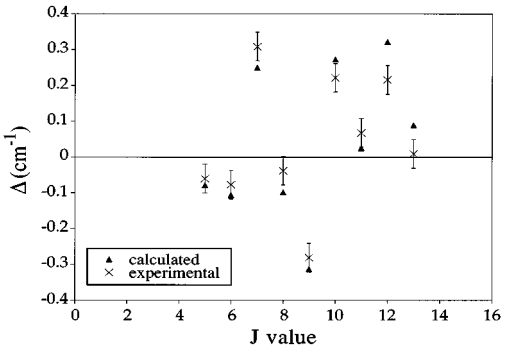


FIG. 10. Comparison between experimental ($\Delta_{exp}$) and calculated ($\Delta_{calc}$) level shifts near the perturbation in the $E\ ^1\Pi$, $v=1$ state. $\Delta_{exp}$ is the difference between observed term energy and the value given by the least square fitting procedure resulting in the constants of Table I. $\Delta_{calc}$ is defined as the difference between term energies calculated without ($V_2\neq0$) and with interaction ($V_2=0$).

$$\begin{pmatrix} E^1\Pi - i\frac{\Gamma_E}{2} & 0 & V^{SO} & 0 \\ 0 & k_{22} - i\frac{\Gamma_k}{2} & k_{12} & k_{02} \\ V^{SO} & k_{21} & k_{11} - i\frac{\Gamma_k}{2} & k_{01} \\ 0 & k_{20} & k_{10} & k_{00} - i\frac{\Gamma_k}{2} \end{pmatrix}. \tag{14}$$

Here, $\Gamma_E$ and $\Gamma_k$ represent the natural linewidths, determined by radiative and predissociative decay, however, excluding the accidental predissociation effects, of the $E\ ^1\Pi$ and $k\ ^3\Pi$ state respectively. As a starting value for $\Gamma_E$ value we chose 0.053 $cm^{-1}$, corresponding to a reported lifetime for the $E\ ^1\Pi$, $v=1$ state of $\tau=10^{-10}$ s.[4] $\Gamma_k$ was then fitted to the experimental data via the following procedure. From diagonalization of the matrix for a specific $\Gamma_k$ values for the linewidth $\Gamma$ of each $J$ state as well as the singlet character $c_E$ of the wave function (both listed in Table VII) are derived. Values for the intensity ratio $\eta_{calc}$ were calculated with Eq. (5) and compared in a least-squares fit to the values of $\eta_{exp}$ as listed in Table VI. In this way an optimized value for $\Gamma_k$ is found at 0.7 $cm^{-1}$, which corresponds to a lifetime of about $\tau=8\times10^{-12}$ s. Experimental and calculated values of $\eta$ are compared in Fig. 11. Again satisfactory agreement is found for the perturbation model. The observed intensity of the line attributed to a transition to $k\ ^3\Pi_{0e}$ $J=7$ is off by a factor of 3 when compared to the model. However, at a calculated line broadening of $\Gamma\approx0.6$ $cm^{-1}$ the rate equation model resulting in Eq. (4) is no longer valid and a steeper dependence on the lifetime should hold. Indeed the line is extra weakened in the observed spectrum.

The above fitting procedure is mainly sensitive to the ratio of the two natural linewidths of $E\ ^1\Pi$ and $k\ ^3\Pi$ states for which we determine $\Gamma_{k(v=5)}/\Gamma_{E(v=1)}=13\pm2$. Absolute values can be deduced from the accurate measurement of one particular linewidth of the $R(6)$ and $P(8)$ lines in the $E-X$ (1,0) band. The observed width of 0.49 $cm^{-1}$ is compatible with the calculated linewidth $\Gamma=0.185$ $cm^{-1}$ (Table VII) and an estimated laser bandwidth of $\delta\nu_{laser}=0.38$ $cm^{-1}$ via Eq. (2). From the fact that the observed line broadening effect on the $E\ ^1\Pi$, $v=1$, $J_e=7$ level agrees with the value of the model, it follows that the starting value of $10^{-10}$ s for the lifetime of the $E\ ^1\Pi$ state is correct. From the present analysis we estimate lifetimes of $10\pm5\times10^{-11}$ s for $E\ ^1\Pi$, $v=1$ and $8\pm2\times10^{-12}$ s for $k\ ^3\Pi$, $v=5$.

A similar quantitative analysis, using the matrix diagonalization of Eq. (13) and (14), can be performed on the local perturbations in the $E\ ^1\Pi$, $v=0$ state. For the $J_e=31$ level, perturbed by the $k\ ^3\Pi$, $v=3$ state an interaction parameter of $V^{SO}=0.95$ $cm^{-1}$ is derived. This value depends on the measured splitting (see Table V) between transitions to $J_e=31$ and the perturber level, which is also observed in both 2+1 REMPI and vuv spectra. From the observed line intensities in 2+1 REMPI spectra only an upper bound for the ratio $\Gamma(k\ ^3\Pi,v=3)/\Gamma(E\ ^1\Pi,v=0)\geqslant10$ can be deduced, since Eqs. (4) and (5) are not strictly valid for the case of saturated ionization. In the vuv spectra the $R(30)$ and the perturber component are extremely weak and a value for the linewidth ratio is found with a rather large error: $\Gamma(k\ ^3\Pi,v=3)/\Gamma(E\ ^1\Pi,v=0)=30\pm10$. The line shifts of the $J_e=41$ and $J_e=44$ levels, obtained in 2+1 REMPI spectra, were used to derive a coupling parameter $V^{SO}=1.5$ $cm^{-1}$ for the interaction between $E\ ^1\Pi$, $v=0$ and $k\ ^3\Pi$, $v=4$. Unfortunately, the accuracy of the parameter $V^{SO}$ is limited because the high $J$ energy levels of $k\ ^3\Pi$, $v=4$ state are only approximately known.

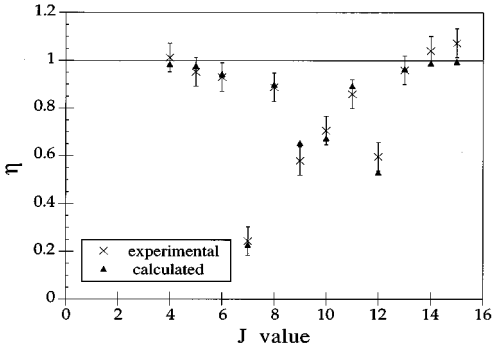


FIG. 11. Comparison of the observed intensity ratios $\eta_{exp}$ and intensity ratios $\eta_{calc}$ calculated in the deperturbation model (see the text) for the accidental predissociation near the $E\ ^1\Pi$, $v=1$, $J=7$ state.

As shown in the spectrum of Fig. 7, similar perturbation phenomena also occur in the $E\ ^1\Pi-X\ ^1\Sigma^+$ (1,0) band of $^{13}C^{16}O$. Transitions corresponding to $J_e=7$ have completely disappeared and the ones related to $J_e=10$ exhibit lower intensities than expected. Unfortunately, molecular constants on $k\ ^3\Pi$, $v=5$ are not available for $^{13}C^{16}O$. Values deduced from an isotopic scaling procedure predict perturbations in the range $J_e=6-12$ but no coincidence for $J_e=7$. As this low-$J$ region is not sensitive to the value of $B$, it may be that $T_{v=5}$ as determined from isotopic scaling is not accurate. The accidental predissociation observed at $J_e=50$ for the $E\ ^1\Pi-X\ ^1\Sigma^+$ (0,0) was located at $J=51$ in the deperturbation analysis (see Fig. 9). If the value for the band origin is lowered to $T_{v=5}=95\ 076.5$ $cm^{-1}$ and the rotational constant taken at $B=1.11$ $cm^{-1}$ a consistent explanation follows with crossings at $J_e=7$ between $E\ ^1\Pi$, $v=1$ and $k\ ^3\Pi_1$, $v=5$ and at $J_e=50$ between $E\ ^1\Pi$, $v=0$ and $k\ ^3\Pi_0$, $v=5$. Other crossing points for $^{13}C^{16}O$ would then occur for $J_e=3$ and 10. This explains the observed intensity decrease at $J_e=10$ as well.

It is interesting to note that only the $^3\Pi_1$ component of the $k\ ^3\Pi$ state couples via spin-orbit interaction to the $E\ ^1\Pi$ state. Nevertheless, all three spin components are found to act as perturbers. For this reason we have calculated the eigenvectors (shown in Fig. 12) of the $k\ ^3\Pi$, $v=5$ state and found, that only at low $J$ values a Hund's case (a) description is valid, in which the upper state is truly $^3\Pi_2$ and so on. Near $J\approx18$ there is a transition from Hund's case (a) to Hund's case (b). At this $J$ value all three state vectors have an equal amount of $^3\Pi_1$ character. Because the rotational constant in $k\ ^3\Pi$, $v=3$ and 4 is larger than in $v=5$ the point of transition to Hund's case (b) lies at even lower $J$. At high $J$ states the upper and lower $^3\Pi$ components, i.e., the states referred

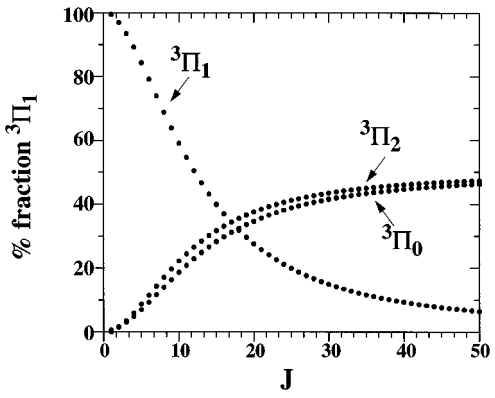


FIG. 12. Calculated $^3\Pi_1$ wave function character of the three triplet components of the $k\ ^3\Pi$, $v=5$ state, using the constants of Ref. 17 and the matrix of Ref. 28. The state denoted as $^3\Pi_2$ is the upper triplet state and the state denoted as $^3\Pi_0$ is the lower triplet state notwithstanding the high contribution of $^3\Pi_1$ character in the wave function at high $J$ values. Note that the amount of $^3\Pi_1$ character determines the strength of the interaction with the $E\ ^1\Pi$ state.

to as $^3\Pi_2$ and $^3\Pi_0$ in this paper, share almost all of the $^3\Pi_1$ character. Also at high $J$ the $^3\Pi$ state of intermediate energy, hitherto referred to as $^3\Pi_1$, has in fact less than 10% of true $^3\Pi_1$ character and may be written as a linear combination of true $^3\Pi_2$ and $^3\Pi_0$ eigenvectors. In the crossings of $E\ ^1\Pi$ and $k\ ^3\Pi$ states, as, e.g., shown in Figs. 8 and 9, only the $^3\Pi_1$ character of the perturber state gives rise to an accidental predissociation effect. This explains why $J_e=29$ and $J_e=42-43$ in $E\ ^1\Pi$, $v=0$ are not affected. The $J_e=3$ level of $E\ ^1\Pi$, $v=1$ in $^{13}C^{16}O$ is nearly coincident with a $^3\Pi_0$ component, which is for this low $J$ value indeed almost purely $^3\Pi_0$ and therefore does not cause an accidental predissociation.

## VI. DISCUSSION AND CONCLUSION

In the present work new accidental predissociations in the $E\ ^1\Pi$, $v=0$ state are observed at $J_e=41$, and 44 for $^{12}C^{16}O$ and $J_e=41$, and 50 for $^{13}C^{16}O$, while the known accidental predissociations at $v=0$, $J_e=31$ and $v=1$, $J_{e,f}=7$ were reinvestigated in detail. In previous work of Baker *et al.*[11,17,20] the perturber state causing the two latter predissociations was identified as the $k\ ^3\Pi$ state. Along the same lines the perturbations at $J=41$, 44, and 50 are attributed here as interactions with $k\ ^3\Pi$, $v=4$ and 5. On the basis of accurate vuv measurements a quantitative description of the perturbation is developed, providing excellent agreement with observation of line shifts and line intensities. A spin-orbit interaction between $^1\Pi$ and the $^3\Pi_1$ component of the $k\ ^3\Pi$ state, involving only a single parameter yield this result.

Furthermore, it is explained that an accidental predissociation occurs in $E\ ^1\Pi$, $v=1$ for both $^{12}C^{16}O$ and $^{13}C^{16}O$ at the same $J=7$ level. While for $^{12}C^{16}O$ there is a crossing with the $^3\Pi_0$ component at $J=7$ for $^{13}C^{16}O$ this is the case for the $^3\Pi_1$ component. For $^{12}C^{18}O$ and $^{13}C^{18}O$, where perturbations are found at $J=7$ and $J=6$, respectively,[11] an explanation along the lines presented here is likely to hold.

From the present deperturbation analysis a lifetime for $k\ ^3\Pi$, $v=5$ is obtained: $8\pm2\times10^{-12}$ s. The $k\ ^3\Pi$, $v=5$ state was observed in direct absorption by Baker and Launay,[17] but no lifetime broadening effects for this particular vibronic level were reported. In the high resolution spectroscopic study of Mellinger and Vidal[19] transitions to various levels of the $k\ ^3\Pi$, $v=1$ and $v=2$ states were observed as narrow resonances and from their linewidths the lifetime of the $k\ ^3\Pi$ state was estimated to be larger than $10^{-10}$ s. In the present study only a ratio between lifetimes of $k\ ^3\Pi$, $v=3$ and $E\ ^1\Pi$, $v=0$ is obtained. If the value of $10^{-9}$ s is taken for $E\ ^1\Pi$, $v=0$[4] then a lifetime follows for $k\ ^3\Pi$, $v=3$ of $3\times10^{-11}$ s. Clearly predissociation rates in the $k\ ^3\Pi$ state strongly depend on the vibrational quantum number.

For the $E\ ^1\Pi$, $v=1$ state $J$-dependent lifetimes were derived in the range of the accidental predissociation $J=5-13$. The method of comparing relative line intensities is very sensitive and therefore the values for the lifetimes as listed in the last column of Table VII are rather accurate on a relative scale. Absolute values of these lifetimes could only be determined with an accuracy of 50%.

The $k$ and $E$ states are assumed to be described by orbital configurations $(\cdots)\ 4\sigma^1 5\sigma^2 1\pi^4 2\pi^1$ (Ref. 20) and $(\cdots)\ 4\sigma^2 5\sigma^1 1\pi^4 3p_\pi$, respectively. These configurations differ by more than one orbital, in disagreement with the assumption that the spin-orbit coupling is the cause of the perturbation. As noted by Baker[20] in the study of the interaction between $k\ ^3\Pi$ and $B\ ^1\Sigma^+$ states, the single configuration description is not strictly valid. From several spectroscopic studies a $c\ ^3\Pi$ Rydberg state is known with the same orbital configuration as the $E\ ^1\Pi$ state,[34,35] although only a $v=0$ component has been observed. As discussed by Baker *et al.*[11] perturbations in the $c\ ^3\Pi$ and $k\ ^3\Pi$ states are attributed to electrostatic interactions between these two states. So our model is consistent if we assume that $E\ ^1\Pi$ state interacts by spin-orbit coupling with the isoconfigurational $c\ ^3\Pi$ character of the $k\ ^3\Pi$ state.

Apart from accidental predissociations, due to the coupling with the $k\ ^3\Pi$ state, the $E\ ^1\Pi$, $v=0$ and $v=1$ are believed to undergo an overall predissociation. Eidelsberg and Rostas[4] reported predissociation yields of 89% and 98% for $E\ ^1\Pi$, $v=0$ and $v=1$, respectively. Predissociation of various electronic states in the energy range just above the dissociation limit are attributed to a coupling with the repulsive part of the $D'\ ^1\Sigma^+$ state, that has bound levels at large internuclear distances and lower energies.[36] For the $B\ ^1\Sigma^+$, $v=2$ state a detailed model involving the coupling with $D'\ ^1\Sigma^+$ was worked out,[37] while the $J$- and parity-dependent predissociation of $W\ ^1\Pi$, $v=0$ and $L\ ^1\Pi$, $v=0$ states was also attributed to a heterogeneous coupling with the $D'\ ^1\Sigma^+$ state.[10,38] If the overall predissociation of the $E\ ^1\Pi$, $v=0$ and $v=1$ states would be due to such an interaction with this $D'\ ^1\Sigma^+$ state, then a $J$-dependent interaction is expected with a predissociation rate

$$k_p^{\text{overall}}=k_p^0 J(J+1). \tag{15}$$

At $J=30$ no line broadening is visible in our vuv spectra and we estimate a limit on the natural lifetime broadening of $\Gamma<0.1\ \text{cm}^{-1}$. This would correspond to a predissociation rate

of $k_p^{\text{overall}} = 1.9 \times 10^{10}$ s$^{-1}$ at $J=30$ and a limiting value for the proportionality constant in Eq. (15): $k_p^0 < 2.0 \times 10^7$ s$^{-1}$. As a consequence a predissociation rate of $k_p < 4 \times 10^7$ s$^{-1}$ would be expected for $E\ ^1\Pi$, $J=1$ and this value is far too small to explain the reported predissociation yields of 98% and 89%, if a radiative lifetime on the order of 1 ns is postulated. In conclusion it is not likely that the $D'\ ^1\Sigma^+$ state is responsible for the overall predissociation of the $E\ ^1\Pi$ state. This line of reasoning would hold for any perturber of $^1\Sigma^+$ symmetry.

Absorption cross sections, lifetimes and predissociation yields of the $E\ ^1\Pi$, $v=0$ and 1 states were shown to be of utmost importance for the isotopic fractionation of $^{12}$CO and $^{13}$CO in the interstellar medium.[1] In previous studies the lifetimes of these states were determined with an accuracy of approximately 300% (a factor of 3). Moreover, values for the lifetimes were obtained from experiments without rotational resolution.[2–4] In the present study we have shown that in the $E\ ^1\Pi$, $v=1$ state drastic rotational effects occur exactly in the range of $J$ states that are populated in a room temperature sample ($J=5-15$). In this respect we wish to speculate on the question whether the higher predissociation yield of the $v=1$ state, with respect to $v=0$, may be attributed to accidental predissociation only. In that case the lifetimes of $E\ ^1\Pi$, $v=1$, $J=0-3$ states, populated in the cold environment of the interstellar medium, might be significantly longer than $10^{-10}$ s and the predissociation yield less than the 98% reported.

## ACKNOWLEDGMENTS

The authors wish to thank Peter Hansen (Lund University, Sweden) and Cecilia Larsson (Linköping University, Sweden), who visited the VU within an ERASMUS-student exchange program, for their assistance during the 2+1 REMPI measurements and the data analysis. Paul Hinnen (VU Amsterdam) assisted in the measurements with the vuv laser. We are grateful to J. Rostas (Meudon, France) for helpful discussions and to C. Amiot (Orsay, France) for critically reading the manuscript. One of the authors (P.C.) received support from EC (Grant No. ERB-4001-GT-931480) and NATO (OTAN-9B/93/FR) for his stay in Amsterdam.

[1] E. F. van Dishoeck and J. H. Black, Astrophys. J. **334**, 771 (1988).
[2] Y. P. Viala, C. Letzelter, M. Eidelsberg, and F. Rostas, Astron. Astrophys. **193**, 265 (1988).
[3] C. Letzelter, M. Eidelsberg, F. Rostas, J. Breton, and B. Thieblemont, Chem. Phys. **114**, 273 (1987).
[4] M. Eidelsberg and F. Rostas, Astron. Astrophys. **235**, 472 (1990).
[5] M. Eidelsberg, J. J. Benayoun, Y. Viala, and F. Rostas, Astron. Astrophys. Suppl. **90**, 231 (1990).
[6] G. Stark, K. Yoshino, P. L. Smith, K. Ito, and W. Parkinson, Astrophys. J. **369**, 574 (1991).
[7] G. Stark, P. L. Smith, K. Ito, and K. Yoshino, Astrophys. J. **395**, 705 (1992).
[8] G. Stark, K. Yoshino, P. L. Smith, J. R. Esmond, K. Ito, and M. Stevens, Astrophys. J. **410**, 837 (1993).
[9] P. F. Levelt, W. Ubachs, and W. Hogervorst, J. Chem. Phys. **97**, 7160 (1992).
[10] K. S. E. Eikema, W. Hogervorst, and W. Ubachs, Chem. Phys. **181**, 217 (1994).
[11] J. Baker, J. L. Lemaire, S. Couris, A. Vient, D. Malmasson, and F. Rostas, Chem. Phys. **178**, 569 (1993).
[12] J. J. Hopfield and R. T. Birge, Phys. Rev. **29**, 922 (1927).
[13] S. G. Tilford, J. T. Vanderslice, and P. G. Wilkinson, Can. J. Phys. **43**, 450 (1965).
[14] J. D. Simmons and S. G. Tilford, J. Mol. Spectrosc. **49**, 167 (1974).
[15] P. Klopotek and C. R. Vidal, J. Opt. Soc. Am. B **2**, 869 (1985).
[16] C. Amiot, J.-Y. Roncin, and J. Vergès, J. Phys. B **19**, L19 (1986).
[17] J. Baker and F. Launay, J. Mol. Spectrosc. **165**, 75 (1994).
[18] B. N. Wan and H. Langhoff, Z. Phys. D **21**, 245 (1991).
[19] A. Mellinger and C. R. Vidal, J. Chem. Phys. **101**, 104 (1994).
[20] J. Baker, J. Mol. Spectrosc. **167**, 323 (1994).
[21] M. Hines, H. A. Michelsen, and R. N. Zare, J. Chem. Phys. **93**, 8557 (1990).
[22] J. Cariou and P. Luc, *Atlas du spectre d'Absorption de la Molecule de Tellure* (CNRS, Paris, 1980).
[23] S. Gerstenkorn and P. Luc, *Atlas du spectre d'Absorption de la Molecule de l'Iode entre 14 800–20 000 cm$^{-1}$* (CNRS, Paris, 1978).
[24] S. Gerstenkorn and P. Luc, Rev. Phys. Appl. **14**, 791 (1979).
[25] G. Herzberg, *Molecular Spectra and Molecular Structure, Vol I: Spectra of Diatomic Molecules* (Van Nostrand, New York, 1950).
[26] S. N. Dobryakov and Y. S. Lebedev, Sov. Phys. Dokl. **13**, 873 (1969).
[27] W. Ubachs, G. Meijer, J. J. ter Meulen, and A. Dynamus, Chem. Phys. **84**, 3032 (1986).
[28] G. Guelachvili, D. De Villeneuve, R. Farrenq, W. Urban, and J. Vergès, J. Mol. Spectrosc. **98**, 64 (1983).
[29] R. Kepa, M. Knot-Wisniewska, and M. Rytel, Acta Phys. Pol. A **48**, 819 (1978).
[30] R. Kepa, Acta Phys. Hung. **60**, 227 (1986).
[31] J. M. Brown and A. J. Merer, J. Mol. Spectrosc. **74**, 488 (1979).
[32] H. Lefebvre-Brion and R. W. Field, *Perturbations in the Spectra of Diatomic Molecules* (Academic, London, 1986).
[33] C. Cohen-Tannoudji, B. Diu, and F. Laloë, *Quantum Mechanics*, Vol. I (Wiley, Paris, 1977).
[34] T. Rytel and M. Rytel, Acta Phys. Hung. **55**, 69 (1984).
[35] T. Rytel and M. Rytel, Acta Phys. Hung. **58**, 355 (1986).
[36] G. L. Wolk and J. W. Rich, J. Chem. Phys. **79**, 12 (1983).
[37] W.-Ü. L. Tchang-Brillet, P. S. Julienne, J.-M. Robbe, C. Letzelter, and F. Rostas, J. Chem. Phys. **96**, 6735 (1992).
[38] M. Drabbels, J. Heinze, J. J. ter Meulen, and W. L. Meerts, J. Chem. Phys. **99**, 5701 (1993).